



MULTI-DIRECTIONAL SHAKE TABLE REAL-TIME HYBRID SIMULATIONS OF FLOOR ISOLATION SYSTEMS IN BUILDINGS

E. Villalobos Vega¹, P.S. Harvey Jr.², J.M. Ricles³, L. Cao³, F. Malik³ & T. Marullo³

¹ University of Oklahoma, Norman, USA, esteban.villalobos@ou.edu
² University of Oklahoma, Norman, USA
³ Lehigh University, Bethlehem, USA

Abstract: Seismic resiliency includes the ability to protect the contents of mission-critical buildings from becoming damaged. The contents include telecommunication and other types of electronic equipment in mission-critical data centres. One technique to protect sensitive equipment in buildings is the use of floor isolation systems (FIS). Multi-directional shake table real-time hybrid simulation (RTHS) is utilized in this paper to validate the performance of full-scale rolling pendulum (RP) bearings, incorporating multi-scale (building-FIS-equipment) interactions. The analytical substructure for the RTHS included 3D nonlinear models of the building and isolated equipment, while the experimental substructure was comprised of the FIS. The RTHS test setup consisted of the FIS positioned on a shake table, where it is coupled to the analytical substructure and subjected to multi-directional deformations caused by the building's floor accelerations and equipment motion from an earthquake. Parametric studies were performed to assess the influence of different building lateral load systems on the performance of the FISs. The lateral load resisting systems included buildings with steel moment resisting frame (SMRF) systems and with buckling restrained braced frame (BRBF) systems. Each building type was subjected to multi-directional ground motions of different sources and hazard levels. Details of the experimental test setup, RTHS test protocol and main preliminary results on the multi-directional testing of an RP-based FIS are described. Challenges in conducting the multi-axial RTHS, including the nonlinear kinematics transformation, adaptive compensation for the actuator-table dynamics, along with the approaches used to overcome them are presented. The acceleration and deformation response of the isolated equipment is assessed to demonstrate the effectiveness of the FIS in mitigating the effects of multi-directional seismic loading on isolated equipment in mission-critical buildings.

1 Introduction

Earthquakes can heavily damage civil structures causing great economic and, in the worst cases, human losses. Several design strategies have been developed to minimize and mitigate the impact of the forces this natural hazard imposes on structures (Christopoulos and Filiatrault, 2006), such as isolating an entire building (Warn and Ryan, 2012). Floor isolation systems (FISs) are gaining popularity over other isolation techniques as they have shown to be a valuable approach for protecting essential building contents, besides facilitating and expediting the post-event functionality of the structure, and consequently, of business operation (Figure 1(a)). FISs are designed under the premise that an object (e.g., telecommunications apparatus, medical equipment, sculptures, a raised floor of a building, etc.) can be decoupled (isolated) from the rest of a structure

and its respective disturbances (Figure 1(b)). Thus, these systems decrease the transmitted vibrations and ultimately protect sensitive and critical objects from damaging effects.



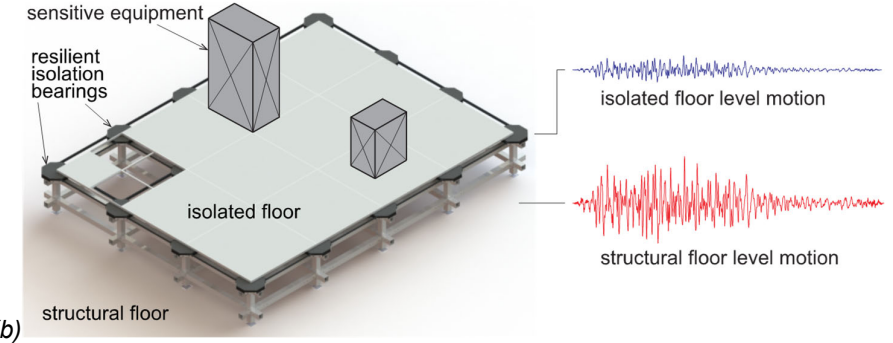


Figure 1. (a) Damage in a data centre after an earthquake (WorkSafe Technologies, Inc., 2021), and (b) schematic of resilient multi-functional FIS concept.

FISs composed of full-scale rolling pendulum (RP) bearings under multi-directional in-plane (X–Z– θ) loading are studied in this paper. To do so, a new real-time cyber-physical structural systems multi-directional shake table at the NHERI Lehigh Experimental Facility (Cao et al., 2020) was constructed and used, which was also used for controlled-displacement characterization tests. Real-time hybrid simulation (RTHS) combines numerical and experimental subsystems into a single simulation technique in real-time (Nakashima, 2020). Thus, by implementing multi-directional RTHS tests (Figure 2), it is possible to numerically model buildings and equipment while only physically testing an isolation unit, as well as to accurately measure the effect of interactions between the former and the latter. By accounting for any possible movement in the plane through the use of the shake table, more realistic and complex studies of the RP isolation system, for instance, bi-directional earthquake excitation and torsional effects, can be performed.

2 Analytical formulation

To evaluate the real-scale RP isolation system's performance under bi-directional earthquake excitation, two structural systems, the 3-story (LA3) steel moment resisting frame (SMRF) building (Figure 3(a)) designed for the SAC Joint Venture project (see Ohtori et al. (2004), Luco (2002), and SAC Joint Venture (2000) for additional details), and the 3-story (3v) buckling restrained braced frame (BRBF) with the chevron-braced (inverted-V-braced) configuration (Figure 3(b)) from Sabelli (2001), were used.

Each building was modeled in 3D using a master node to define diaphragm action at each floor level. The model included $P-\Delta$ effects to account for geometric nonlinearities by means of a lean-on column slaved to each master node. The results from numerical simulations using OpenSees models (McKenna and Fenves, 2000) were compared to results using HyCoM-3D models (Ricles et al., 2021), the latter of which is used to create the models for the RTHS numerical substructure. The comparisons included obtaining identical natural frequencies from those reported in previous studies (Ohtori et al., 2004; Luco, 2002; Sabelli, 2001) in addition to time history response analysis results.

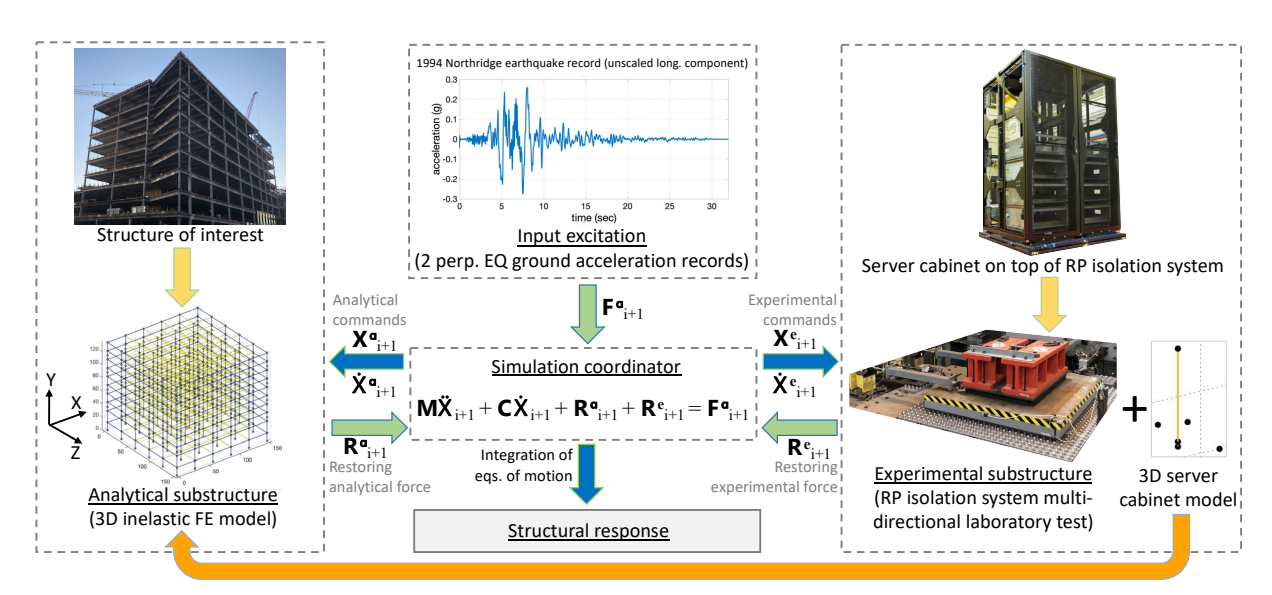


Figure 2. Multi-directional RTHS scheme.

Inelastic explicit force-based fiber beam-column elements were used to model the girders of the SMRFs. These explicit formulated elements were integrated using a Gauss-Lobatto scheme with 5 integrations points along each element. The element formulation includes a fixed number of iterations at the element level to satisfy compatibility at the element ends and element local equilibrium by reducing unbalanced internal member section forces at the element's integration points and the associated element deformations. Any unbalanced section forces that exist after a fixed number of iterations are carried over to the next time step, avoiding iterating in a nondeterministic manner that prevents the element's state determination from being completed within each time step of a RTHS. See Kolay and Ricles (2018) for complete details of the element formulation. In the case of the BRBF, six explicit inelastic force-based co-rotational elements were used to model each brace, specifying a geometric initial imperfection value of 0.002 times the brace's length in the form of a half-sine wave. Elastic elements were used to model the columns and gravity system's beams since these members are expected to remain elastic during an earthquake.

For both structures, Rayleigh proportional damping based on initial elastic stiffness was used with a viscous damping of 2% assigned at the fundamental period of each building model and at a period of 0.2 sec, as established during the SAC Joint Venture project (Luco, 2002). In the RTHS, the MKR- α algorithm (Kolay and Ricles, 2014; Kolay et al., 2015; Kolay and Ricles, 2016; Kolay and Ricles, 2019) was used to integrate the equations of motion in real time. The MKR- α algorithm is a model-based explicit dissipative integration algorithm with controlled numerical damping. The spectral radius ρ^*_∞ , which controls numerical damping, was set to a value of 0.5 for all simulations (Kolay and Ricles, 2019). For the OpenSees models, the HHT- α (Hilber-Hughes-Taylor) implicit integration algorithm with a 0.8 value of α (Hilber et al., 1977) was used as the integration scheme (McKenna and Fenves, 2000) for the numerical validation studies of the HyCoM-3D models.

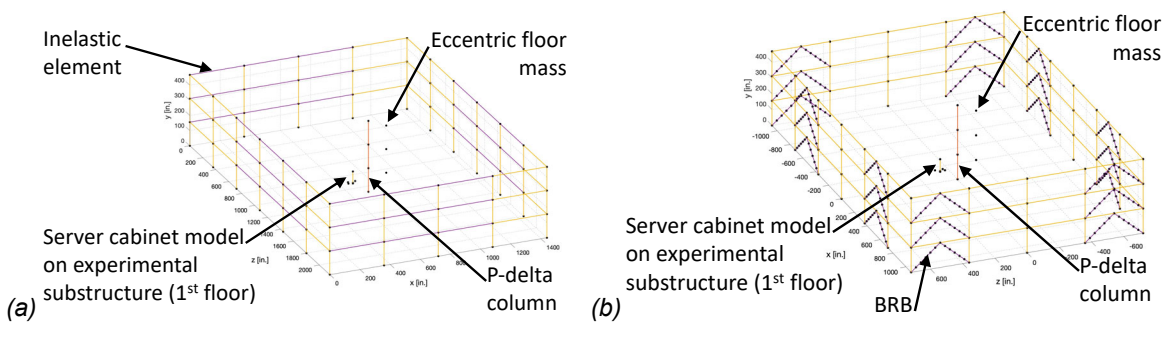


Figure 3. 3D non-linear steel building models: (a) SMRF, and (b) BRBF.

An ensemble of representative risk-targeted bi-directional earthquake records was chosen for the RTHS, following the procedure of Sections 16.2.3.2 and 16.2.4 in ASCE 7-22 (ASCE, 2022a) for scaling each ground motion for nonlinear response history analysis. First, a target 5%-damped MCE_R response spectrum was defined for the Los Angeles financial district (lat. 34.05, long. -118.26) (ASCE, 2022b). This location was selected as the build site because of the site's importance, building density, and high seismic risk zone.

The NGA-West2 ground motion database and online tool for amplitude scaling (PEER, 2022) were used to scale the ground motions. Various parameters were used to arrive at the selection of 13 near-fault, 3 far-field, and 7 near-fault pulse-like (Haselton et al., 2017) bi-directional scaled records. The parameters included: spectral ordinate RotD100; predominantly fault mechanisms identified for the Los Angeles area (strike-slip and thrust) (Hauksson, 1990); magnitudes between 6 and 7.9, and only one record per earthquake.

A deaggregation analysis of the location showed that the contribution of far-field earthquakes to the seismicity was mainly from the service level earthquake (SLE) hazard level. The design basis earthquake (DBE) and maximum credible earthquake (MCE_R) hazard levels caused by near-fault events mainly contributed to the site's seismicity (Mercado et al., 2019; USGS, 2022). Therefore, priority was given to near-fault ground motion records, which is a result expected for Southern California (Haselton et al., 2017). Note that the SLE, DBE, and MCE_R have a probability of exceedance of 50%, 10%, and 2% in 50 years, respectively (Mercado et al., 2019; USGS, 2022).

3 Experimental procedure

A single full-scale (4 RP bearings) OCTO-Base[™] isolation system from WorkSafe[™] Technologies was used as the prototype isolation system. Each RP isolation unit consists of two steel plates (upper and lower) that act as rolling surfaces, each with an interior radial conical shape and exterior radial constant slope shape. The plates are covered by either an elastomeric coating (QuakeCoat[™]) treatment surface or uncovered consisting of a bare steel surface. A steel ball rolls in between the surfaces of two plates. Figure 4(a) shows a simplified schematic of the experimental substructure test setup for the RTHS. The bottom component of the isolation system is attached to the shake table, which is mounted on top of the table's roller-bearing bed and free to move and rotate in the plane by means of 3 actuators (2 in the *X*-direction and 1 in the perpendicular *Z*-direction, see Figure 4).

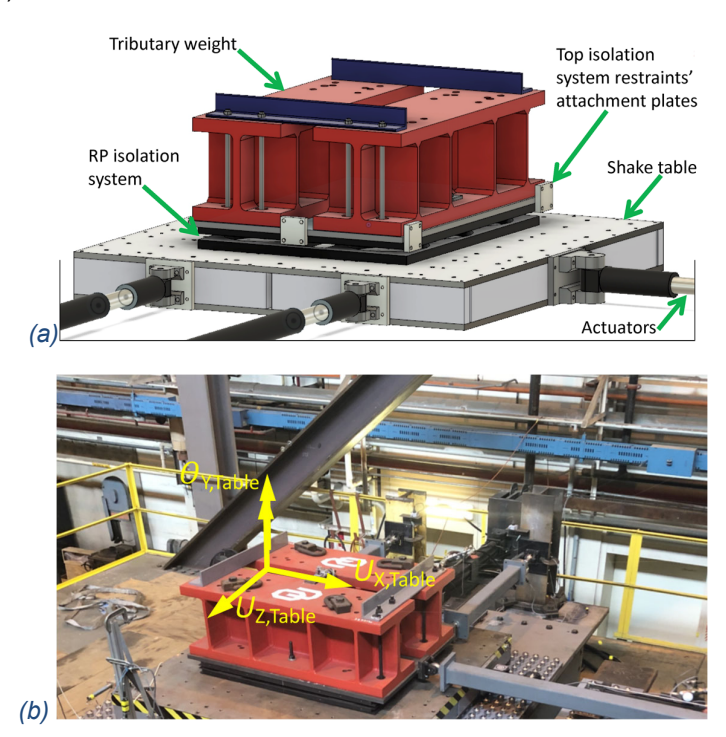


Figure 4. (a) Schematic of test setup using the shake table, and (b) photograph of RTHS experimental setup at the NHERI Lehigh Experimental Facility (Cao et al., 2020).

Attached to the top plate is an assembly composed of I-beams and transfer plates connected by angles and threaded-rod bolts, which represent the 17.9 kN tributary weight acting on the isolation system. In addition, restrainers with load cells were used to restrain the movement of the upper plate while measuring the restoring forces in the X- and Z- directions as well as any moment about the Y-axis associated with the twist of the bottom plate. Because of the concave geometry of the isolation unit's rolling surfaces, a horizontal movement produces a vertical displacement of the top plate. In order to not restrain this vertical movement, spherical bearings were located at both ends of the restrainers and their length was designed to be long enough to make vertical motions negligible in terms of requiring no kinematic corrections applied to the load cell readings.

In standard shake table tests, actions are imposed at the bottom and the isolation system is completely free to move. For this study, it was more meaningful to restrict the top component from the horizontal movement for two reasons: first, it allowed imposing controlled displacement motions according to specific desired characterization tests; and second, the uniaxial load cells directly measure the restoring forces at the top plate that are needed by the integration algorithm for solving the equations of motion. Figure 4(b) shows a photograph of the test set-up for the experimental substructure. The in-plane restraints are shown to run parallel to the actuators, attached to the top plate of the isolation system.

In addition to the instrumentation already discussed, 3 accelerometers on the shake table measured the inplane acceleration of the isolation system, and 1 accelerometer and 2 LVDTs were used to measure the vertical motion on the top of the isolation system. Due to the inherent multi-directional characteristics of the tests, a nonlinear kinematic transformation was necessary to correct the nonlinear motions of the shake table (Mercan et.al., 2009), using string pots to measure the position of the table.

As mentioned before, controlled displacement characterization tests were performed to study the response of the isolation system subjected to a variety of multi-directional conditions (Becker and Mahin, 2012). Specifying different frequencies and velocities, a variety of table motions—that included steady amplitude incremental sine motions, circular motions, T-like motion patterns, square-shaped patterns, triangular patterns, figure-8 patterns, among other shapes with and without rotations—were developed to test and capture the performance of the shake table and the isolation system. In total, 19 characterization tests were performed with these table motions prior to performing the RTHS study.

A campaign of RTHS tests was performed, defined by an extensive experimental test matrix. The matrix incorporated a combination of the building models (LA3 MRF and 3v BRBF models), space location within each structure (first-2 floors), earthquake records (far-field, near-fault without a pulse, and near-fault pulse-like), hazard levels (SLE, DBE, and MCE_R), and RP plates surface treatments.

4 Selected results

Selected results from the RTHS involving the 1983 Coalinga earthquake record ("Cantua Creek School" station) at the SLE hazard level (far-field) is presented. For this case, the RP bearing is located eccentrically from the center of gravity of the 2nd floor of the SMRF. The results presented herein corresponds to the steel plates with the elastomeric coating surface treatment.

Shown in Figure 5(a) and (b) are the normalized shear resisting force V_x/W and V_z/W of the RP bearing for the X- and Z-directions, respectively. V_x , V_z , and W are the shear force in the X- and Z-directions, and the weight of the equipment, respectively. The plots show a high concentration of force-deformation behaviour within the internal conical shape of the top and bottom plates (i.e., when the deformation is less than +/-120mm) of the RP system. In the Z-direction (Figure 5(b)), it can be seen at the origin of the plot that the force-displacement relationship shows a higher stiffness. This effect can be explained by the fact that due to the weight W acting on the system, the steel balls form a divot while at the rest position, adding an additional shape with a higher curvature in the center of the plate.

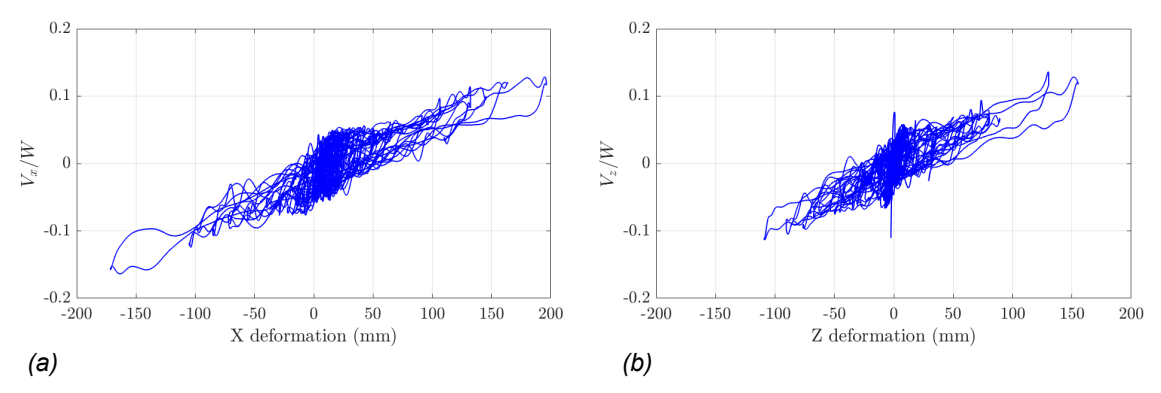


Figure 5. RP normalized force in the (a) X-direction and (b) Z-direction.

The hysteresis that can be seen in the plots is due to the coating surface treatment, which adds energy dissipation capacity to the system, helping additionally to dimmish the seismic demand capacity. The plots show some excursions beyond the conical surface (i.e., beyond a deformation of +/-120mm) to the constant slope portion of the plates. This is seen particularly in the *X*-direction.

Although the plots in Figure 5(a) and (b) help to visualize the behavior of the RP system and compare the behavior in each direction, is important to highlight the multi-directional characteristic of the RTHS tests under perpendicular earthquake records in the plane. Figure 6(a) shows the deformation of the RP system in the X-Z plane, where it can be seen again the higher demand is in the X-direction. Finally, as mentioned before, because of the conical profile of the plates, even though there is no vertical seismic demand during the tests, the steel balls and the top component of the RP system move vertically as a function of the horizontal displacement, where this phenomenon is seen in Figure 6(b).

Shown in Figure 7(a) and (b) are the total (i.e., absolute) horizontal acceleration time histories in the X- and Z-directions at the 2^{nd} floor level and at the top of the numerical substructure for the equipment located on top of the experimental RP system. In Figure 7(b) it can be seen that although the seismic demand in the X-direction was higher, the maximum magnitude of equipment absolute acceleration values are higher in the Z-direction. This is related to the higher forces observed at the beginning of the test due to the divot on the surface treatment, as discussed earlier. A significant reduction in the acceleration values at the top of the analytical substructure of the server cabinet is seen in Figure 7(b). Relative to the floor accelerations, the reduction in the equipment accelerations is 81.3% and 68.9% in the X- and Y-directions, respectively.

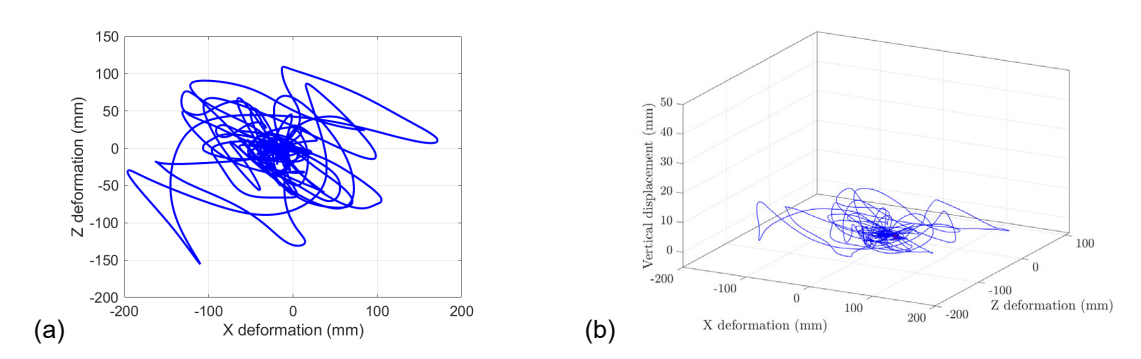


Figure 6. (a) RP deformation in X-Z plane, and (b) equipment vertical displacement vs RP deformation in the X-Z plane.

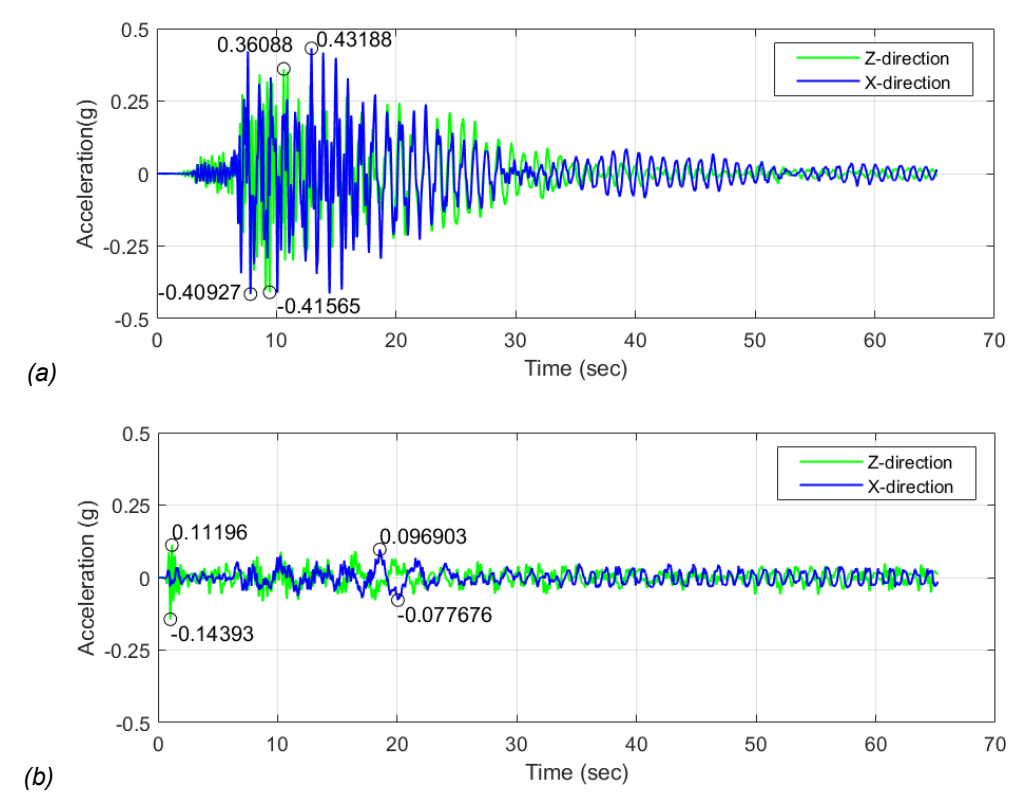


Figure 7. Total accelerations in X- and Z-directions with the maximum magnitudes of absolute acceleration values of each component highlighted: (a) floor total acceleration, and (b) equipment total acceleration.

5 Conclusions

Protecting essential building contents in order to facilitate the post-event functionality of business operations has become a major concern in recent years, where the use of RP-based FISs can play an important role. Therefore, determining and validating their multi-directional performance under realistic dynamic excitation conditions is key for their implementation in design applications.

Preliminary results obtained using RTHS show that the RP isolation system can effectively isolate sensitive mission-critical equipment under multi-directional ground motions.

The use of the multi-directional shake table at the NHERI Lehigh Experimental Facility for this and future projects will facilitate improving the level of resiliency of multi-directional devices that in the past were possible to study only in one direction.

6 Acknowledgments

This material is based upon work supported by the National Science Foundation (NSF) under Grant Nos. CMMI-1663376, OIA-1929151, and CMMI-1943917. The experiments reported herein were performed at the NHERI Lehigh Experimental Facility, whose operation is supported by a grant from the NSF under Cooperative Agreement No. CMMI-2037771. Additional financial support was provided by the Pennsylvania Infrastructure Technology Alliance (PITA). Any opinions, findings, and conclusions expressed in this paper are those of the authors and do not necessarily reflect the views of the sponsors (the NSF and PITA) acknowledged herein.

7 References

ASCE (2022a). Minimum Design Loads and Associated Criteria for Buildings and Other Structures, American Society of Civil Engineers (ASCE), Reston, VA, ASCE/SEI 7-22 ed., doi: 10.1061/9780784414248.

ASCE (2022b). ASCE 7 Hazard Tool, Online, URL https://asce7hazardtool.online/.

Becker, T.C and Mahin, S.A. (2012). Experimental and Analytical Study of the Bi-Directional Behaviour of the Triple Friction Pendulum Isolator, *Earthquake Engineering and Structural Dynamics*, 41(3): 355–373, doi: 10.1002/eqe.1133.

- Cao, L., Marullo, T., Al-Subaihawi, S., Kolay, C., Amer, A., Ricles, J., Sause, R., Kusko, C. S. (2020). NHERI Lehigh Experimental Facility with Large-Scale Multi-Directional Hybrid Simulation Testing Capabilities, Frontiers in Built Environment, 107(6), doi: 10.3389/fbuil.2020.00107.
- Christopoulos, C. and Filiatrault, A. (2006). *Principles of passive supplemental damping and seismic isolation.* IUSS Press, Pavia, Italy.
- Haselton, C. B., et al. (2017). Response History Analysis for the Design of New Buildings in the NEHRP Provisions and ASCE/SEI 7 Standard: Part I Overview and Specification of Ground Motions, *Earthquake Spectra*, 33 (2): 373–395, doi:10.1193/032114EQS039M.
- Hauksson, E. (1990). Earthquakes, Faulting, and Stress in the Los Angeles Basin, *Journal of Geophysical Research*, 95(B10): 15,365–15,394, doi: 10.1029/JB095iB10p15365.
- Hilber, H.M.; Hughes, T.J.R.; Taylor, R.L. (1977). Improved Numerical Dissipation for Time Integration Algorithms in Structural Dynamics, *Earthquake Engineering and Structural Dynamics*, 5(3): 283–292, doi: 10.1002/eqe.4290050306
- Kolay, C. and Ricles, J.M. (2019). Improved Explicit Integration Algorithms for Structural Dynamic Analysis with Unconditional Stability and Controllable Numerical Dissipation, *Journal of Earthquake Engineering*, 23(5): 771–792, doi: 10.1080/13632469.2017.1326423.
- Kolay, C. and Ricles, J.M. (2018). Force-Based Frame Element Implementation for Real-Time Hybrid Simulation Using Explicit Direct Integration Algorithms, *Journal of Structural Engineering*, 144(2), doi: 10.1061/(ASCE)ST.1943-541X.0001944.
- Kolay, C. and Ricles, J.M. (2016). Assessment of Explicit and Semi-Explicit Classes of Model-Based Algorithms for Direct Integration in Structural Dynamics, *International Journal of Numerical Methods in Engineering*, 107(1): 49–73, doi: 10.1002/nme.5153.
- Kolay, C., Ricles, J.M., Marullo T.M., Mahvashmohammadi, A., Sause, R. (2015). Implementation and Application of the Unconditionally Stable Explicit Parametrically Dissipative KR-α Method for Real-Time Hybrid Simulation. *Earthquake Engineering and Structural Dynamics*, 44(5): 735–755, doi: 10.1002/eqe.2484.
- Kolay, C. and Ricles, J.M. (2014). Development of a Family of Unconditionally Stable Explicit Direct Integration Algorithms with Controllable Numerical Energy Dissipation, *Earthquake Engineering and Structural Dynamics*, 43(9):1361–1380, doi: 10.1002/eqe.2401.
- Luco, N. (2002). *Probabilistic Seismic Demand Analysis, SMRF Connection Fractures, and Near-Source Effects.* PhD Thesis, Stanford University.
- McKenna, F. and Fenves, G. L. (2000). Open System for Earthquake Engineering Simulation (OpenSees), Pacific Earthquake Engineering Research Center (PEER), University of California, Berkeley, CA, version 2.5.0 ed.
- Mercado, J. A., Arboleda-Monsalve, L. G., Terzic, V. (2019). Seismic Soil-Structure Interaction Response of Tall Buildings, in: Eighth International Conference on Case Histories in Geotechnical Engineering (Geo-Congress 2019), doi:10.1061/9780784482100.013.
- Mercan, O., Ricles, J., Sause, R., Marullo, T. M. (2009). Kinematic Transformations for Planar Multi-Directional Pseudodynamic Testing. *Earthquake Engineering and Structural Dynamics*, 38(01): 1093–1119, doi:10.1002/eqe.886.
- Nakashima, M. (2020). Hybrid simulation: An early history, *Earthquake Engineering and Structural Dynamics*, 49(10): 949–962, doi: 10.1002/eqe.3274.
- Ohtori, Y., Christenson, R. E., Spencer, Jr., B. F., Dyke, S. J. (2004). Benchmark Control Problems for Seismically Excited Nonlinear Buildings, *Journal of Engineering Mechanics*, 130: 366–385, doi: 10.1061/(ASCE)0733-9399(2004)130:4(366).
- PEER (2022). NGA-West2–Shallow Crustal Earthquakes in Active Tectonic Regimes, Online, URL: https://peer.berkeley.edu/research/nga-west-2.

Ricles, J., Kolay, C., Marullo, T. M. (2021). HyCoM-3D: A Program for 3D Nonlinear Dynamic Analysis and Real-Time Hybrid Simulation of 3-D Civil Infrastructure Systems, Tech. Rep., Hybrid Computational Modeling (HyCoM) Program—3D Version 3.8 User's Manual.

- Sabelli, R. (2001). Research on Improving the Design and Analysis of Earthquake Resistant Steel Braced Frames, Tech. Rep. PF2000-9, Earthquake Engineering Research Institute (EERI), Oakland, CA.
- SAC Joint Venture (2000). State of the Art Report on Systems Performance of Steel Moment Frames Subject to Earthquake Ground Shaking, Tech. Rep. FEMA-355C, Washington, DC.
- USGS (2022). Unified Hazard Tool, Online, URL: https://earthquake.usgs.gov/hazards/interactive/.
- Warn, G. P. and Ryan, K. L. (2012). A review of seismic isolation for buildings: Historical development and research needs, *Buildings*, 2: 300–325, doi: 10.3390/buildings2030300.
- WorkSafe Technologies, Inc. (2021). RISK VS ROI, Online, URL: https://worksafetech.com/risk-vs-roi/.